Supporting Information

Impact of Surface Functionalization on Bacterial Cytotoxicity of Single-Walled Carbon Nanotubes

LEANNE M. PASQUINI[a], SARA M. HASHMI[a], TOBY J. SOMMER[b], MENACHEM ELIMELECH[a], JULIE B. ZIMMERMAN[*a,c]

[a] *Department of Chemical and Environmental Engineering, Yale University, New Haven, CT 06520-8286*
[b] *Department of Chemistry, Yale University, New Haven, CT 06520-8107*
[c] *School of Forestry and Environmental Studies, Yale University, New Haven, CT 06520*

Pages S1-S17
Figures S1-S12
Table S1-S4

Materials and Methods

With the exception of hydrazine and diphenylcyclopropyl SWNT, all fSWNTs were prepared by published methods [1-5].

General: SWNTs synthesized by CVD were purchased from Nanostructured & Amorphous Materials Inc., Houston TX (Stock# 1284YJ, 90% SWNTs, 95% CNTs, Lot: 1284-091009). Residual amorphous carbon was removed by heating SWNT powder in an open Petri dish in a furnace (Thermolyne 48000) for 3 hours at 350 °C. Once cooled, the tubes were placed in 12 M HCl (200 mL/g SWNTs) and bath sonicated for 1 hour to remove residual metal catalyst. The tubes were repeatedly filtered and washed with DI until neutral. The resulting acid treated tubes were dried overnight in an open glass Petri dish at 60 °C. These dry oxidized, acid treated SWNTs (starting material) were used for further functionalizations.

Reagents were standard laboratory grade unless otherwise noted. Dioxane was purchased from Mallinckrodt and used without purification after testing negative for peroxides. A Branson 2510R-MT, 100 W, 42 kHz sonicator was used in the synthetic procedures without cooling; the water bath and solvents warmed considerably during sonication. NMR spectra were recorded as heterogeneous suspensions in deuterated solvents on a Bruker Avance 400 MHz spectrometer.

Hydrazine SWNTs. The preparation of hydrazine functionalized SWNTs closely follows the method of Yokoi, et al.[6]. Starting material SWNTs (292 mg, 24.3 mmole carbon) were dispersed in 410 mL of 10 mM aqueous sodium dodecylsulfate (SDS) by bath sonication for one hour at ambient temperature. To the room temperature SWNT suspension was slowly added hydrazine hydrate (2.80 g, 60% in water, 48 mmole, 2.0 equivalents/carbon). The reaction vessel was flushed with argon, sealed with a plastic cap and allowed to stir at room temperature for 3 days. The suspension was diluted with 600 mL dimethylformamide (DMF) and filtered through a 5 μm hydrophilic PTFE membrane (Millipore, JMWP, Omnipore, 47 mm). The fSWNTs were resuspended and filtered thrice with DI water, twice with ethanol, and twice with methanol. The final SWNT buckypaper was dried overnight in a loosely covered Petri dish at 80 °C. Recovery = 246 mg hydrazine SWNTs.

Diphenylcyclopropyl SWNTs. SWNTs are known to be reactive to carbene additions to form cyclopropanated, bridged or insertion adducts [7-9]. Diphenyldiazomethane $Ph_2C{=}N_2$ generates a carbene known to be reactive towards relatively inert materials [10, 11]. It does not appear that the reaction between SWNTs and diphenyldiazomethane has been previously reported. We describe our product as being cyclopropanated without distinguishing it from other possible isomers.

The prepared starting material SWNTs (76 mg, 6.3 mmole carbon) were dispersed in 250 mL dioxane by sonication for one hour. Diphenyldiazomethane was prepared according to the method of Jonczyk and Wlostowska [12]. Benzophenone tosylhydrazone (CAS [4545-20-4], Aldrich Cat. No. 566799, 490 mg, 1.4 mmole, used as received) was dissolved in 6 mL dioxane. To this solution was added 50% aqueous NaOH (0.74 mL, 9.3 mmole, 6.6 equivalents) at room temperature. The vigorously stirred mixture was heated at 90 °C (bath) under argon for one hour. The reaction turned cherry red within the first two minutes. After cooling to room temperature, the bright red organic phase was separated, washed twice with water, dried over $MgSO_4$ and filtered directly into the freshly prepared SWNT suspension. The SWNT-diazo suspension was protected from light (Al foil) and evaporated to dryness on a rotary evaporator

(bath = 25 °C). The dry residue of presumed uniformly diazo coated SWNTs was heated overnight in a cotton plugged flask in an oven at 150 °C. The residue was resuspended in 200 mL dioxane and filtered through a 5 μm hydrophobic PTFE membrane (Millipore, LSWP, Mitex, 47 mm). The filtrate was colorless indicating that there was no soluble diazo compound remaining. The SWNTs were resuspended and filtered twice in dioxane, once in ethanol and once in methanol. The black fSWNT powder was dried overnight at 80 °C. Recovery = 58 mg diphenylcyclopropyl SWNTs. NMR (Figure S1): Phenyl protons from 7-8 ppm are detectable in a suspension of SWNTs in DMSO-d6. The low concentration accounts for the low signal to noise. The heterogeneity of the material accounts for the broad peak shapes.

The presence of 0.53% nitrogen but lack of any sulfur in the XPS of the diphenylcyclopropyl SWNTs precludes the presence of unreacted tosylhydrazone starting material. The nitrogen content may derive from minor side reactions. It is possible that residual metal catalyst (iron and cobalt "M" are present in our SWNTs) reacts with the diphenyldiazomethane in a known fashion to form a diazenido metal derivative $M{=}N{-}N{=}C(Ph)_2$. Organometallic diazenido complexes are stable entities. Even if the more inorganic metal species contaminating the SWNTs is not as stable as the organometallic counterpart, it is likely to decompose to the more stable metal nitride (M_xN_y, e.g., FeN) as temperatures reach 150 °C. Although diphenyldiazomethane normally reacts as a free carbene, it is also possible that a first formed diphenylpyrazole intermediate, arising from a [3+2] cycloaddition rather than a direct carbene insertion, does not extrude nitrogen to form a cyclopropane or other nitrogen-free product, even at 150 °C. Both C-N N1s and Fe-N N1s XPS signals are known to occur at around 400 eV. Our XPS data near 400 eV does not allow us to distinguish the metal nitride from the pyrazole. Although the metal nitride is preferred on grounds of stability, a definitive assignment cannot be made at this time.

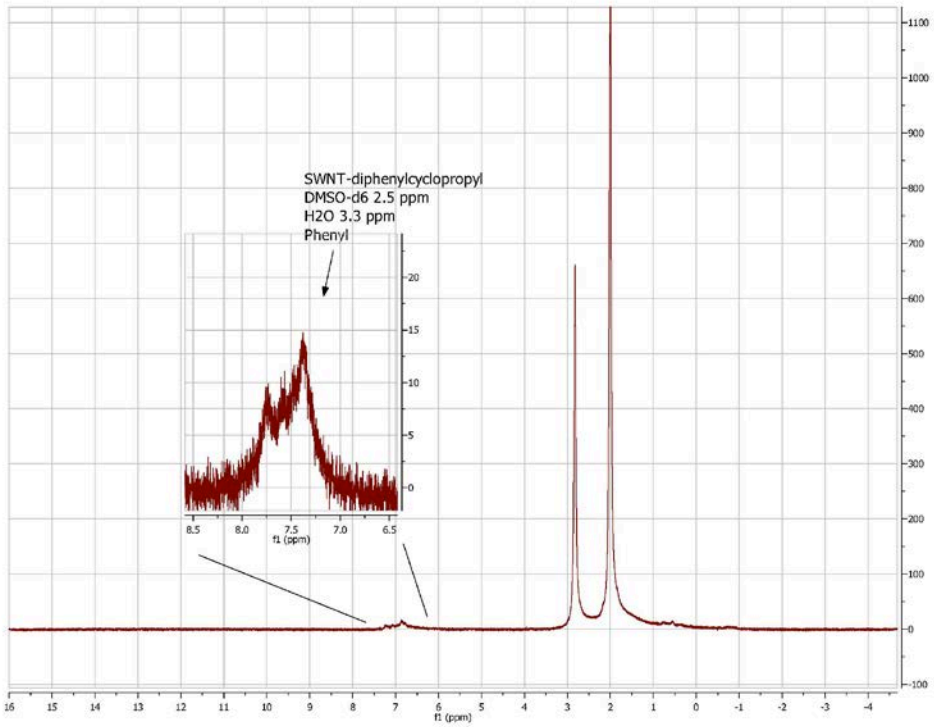

Figure S1. Proton NMR of diphenylcyclopropyl SWNT **1e** in DMSO-d6.

Also included here are proton NMR spectra of other CH containing SWNTs **1a**, **1c**, **1d**, and **1f**. We did not expect to see exchangeable NH or OH protons in standard NMR solvents at very low concentrations. n-Propylamine SWNT **1a** displays several surprisingly sharp peaks from 2-4 ppm indicative of aminomethylenes experiencing different shielding environments along a complex SWNT backbone or within a SWNT cluster (Figure S2). The CH_2 peaks are obscured by H_2O. There is a broad triplet-like signal at 0.9 ppm indicative of the terminal CH_3. Phenylhydrazine SWNT **1c** displays several aryl-H from 6.5-8.2 ppm (Figure S3). Phenyl SWNT **1d** shows characteristic phenyl and biphenyl protons from 7-8.5 ppm (Figure S4). Butyl SWNT **1f** shows a broad alkyl peak from 1-3 ppm (Figure S5). Along with XPS, Raman and other data, these NMR support the conclusion that each functional group was successfully incorporated into the SWNT.

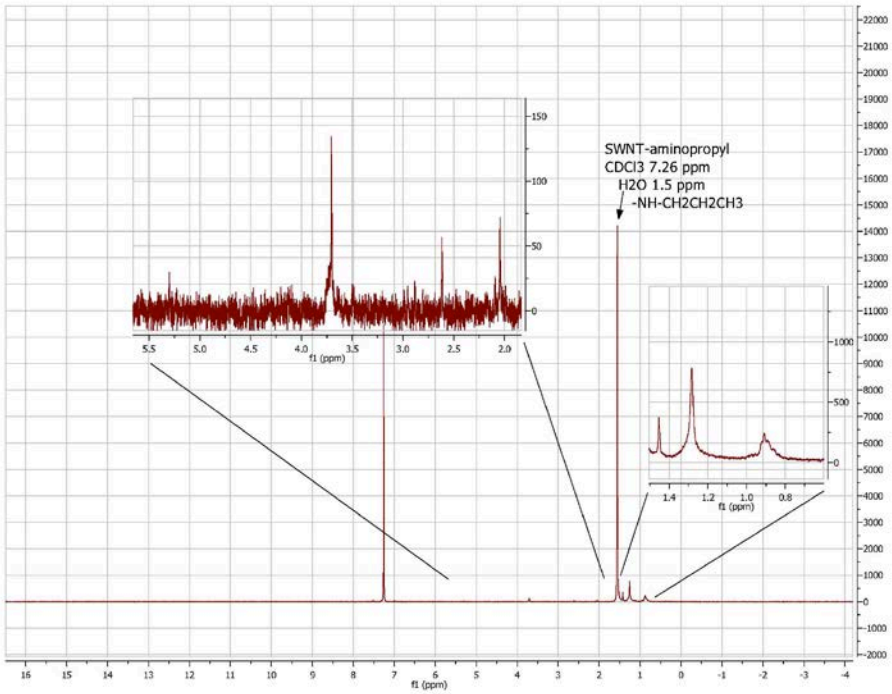

Figure S2: Proton NMR of n-propylamine SWNT **1a** in $CDCl_3$.

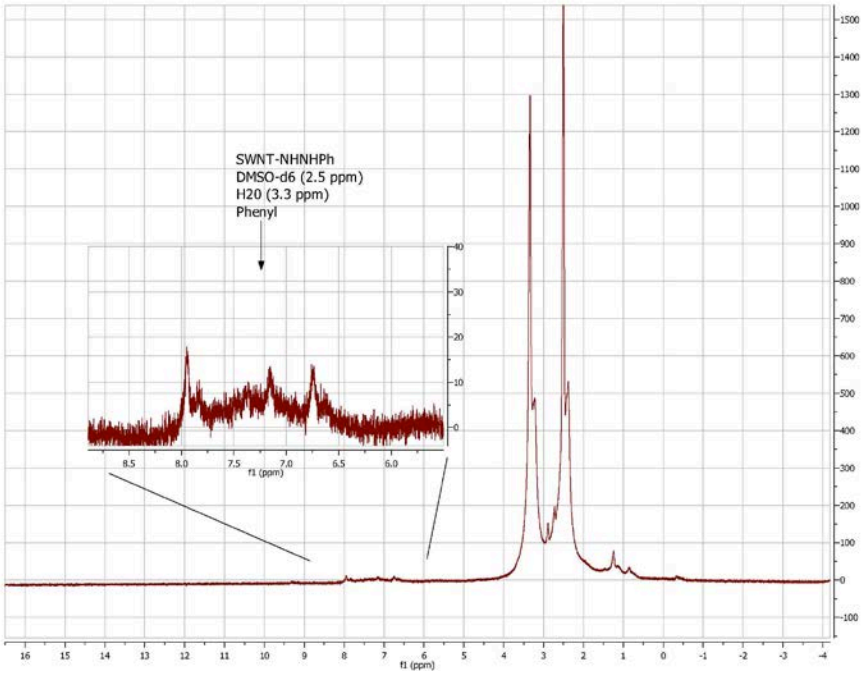

Figure S3. Proton NMR of phenylhydrazine SWNT **1c** in DMSO-d6.

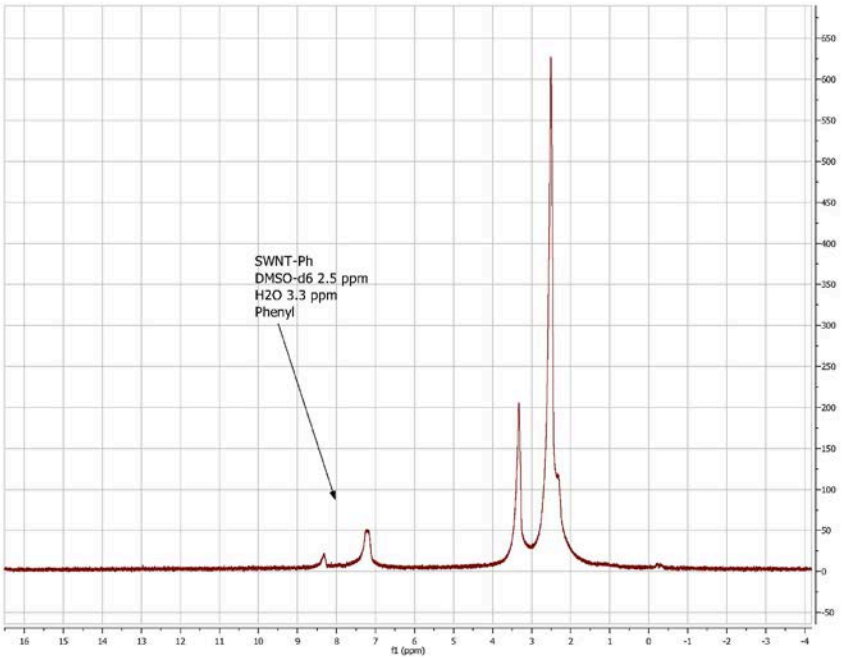

Figure S4. Proton NMR of phenyl-SWNT **1d** in DMSO-d6.

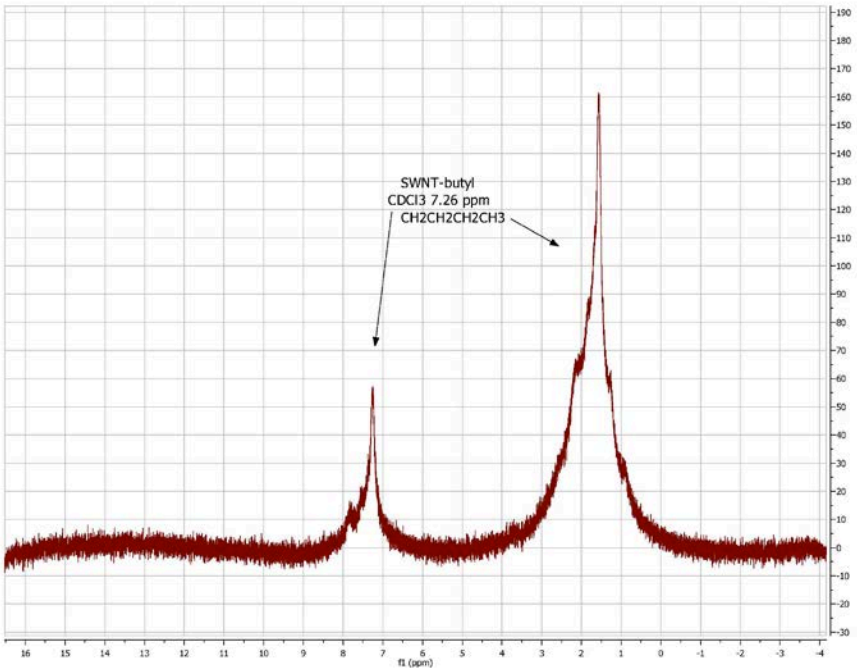

Figure S5. Proton NMR of butyl-SWNT **1f** in $CDCl_3$.

Cytotoxicity Assay. To obtain a percent loss of cell viability for each sample of interest, the ratio of compromised cells to total cells is measured. Fluorescent dyes that bind to cellular DNA are utilized to identify viable and nonviable cells. 4',6-Diamidino-2-phenylindole dihydrochloride (DAPI), a blue emitting dye, will diffuse through all cells while propidium iodide (PI), a red emitting dye, will only penetrate those cells that have compromised cell walls.

E. coli were grown in Luria-Bertani broth (LB broth, BD, Sparks, MD) at 37 °C (VWR Scientific Products Incubator, 150 rpm). After harvesting during exponential growth phase, cells were pelleted by centrifuge, washed twice and resuspended in 0.9% NaCl (isotonic saline) solution. The bacterial suspension was diluted to obtain a 10 mL suspension of 1×10^6 cells/mL to be used in the toxicity assay.

For the toxicity assay, 0.5 mg of each SWNT sample was dispersed in 20 mL DMSO by probe sonication for 15 minutes. The samples were immediately filtered through a 5.0 μm pore PTFE membrane (Millipore, JMWP 04700) using a Gast vacuum pump to form a SWNT deposit layer. Samples were washed with 250 mL ethanol to remove residual DMSO and 350 mL DI water to remove residual ethanol, both of which are increased amounts from those previously reported to ensure full removal of residual solvents [13, 14]. The SWNT coated membranes were stored in a sterilized Petri dish with isotonic saline while the bacterial solution was prepared. A black nitrocellulose membrane (0.45 μm, Millipore, HABP 04700) was used for the experimental control.

A live-dead fluorescent cytotoxicity assay, similar to the one used in previous studies [13, 15], was utilized to obtain relative percent cell viability loss of *E. coli* K12 exposed to pristine and fSWNT samples. The prepared bacterial suspension was filtered through a control membrane and SWNT-coated filters using a vacuum pump. The samples were placed in a sterilized Petri dish, submerged in isotonic saline, the Petri dish covered in aluminum foil, and

incubated at 37 °C for 30 minutes. After 30 minutes, the solution was decanted and approximately 2-3 mL of PI (Invitrogen, 3.14 μM final concentration, excitation/emission at 535 nm/617 nm) was added to each Petri dish, avoiding prolonged exposure to light. Petri dishes were re-covered with aluminum foil and incubated for an additional 15 minutes to allow cellular binding of PI. After 15 minutes, the PI was decanted and the samples washed gently with saline to remove residual PI before adding approximately 2-3 mL of DAPI (Invitrogen, 49.4 μM final concentration, 358 nm/461 nm). After 5 minutes in the dark, the DAPI was decanted and the samples washed gently with saline. Samples were placed on a glass slide for imaging using an epifluorescence microscope (Olympus M14) with a U filter (364 nm/440 nm) to detect cells stained with PI and DAPI, and an IB filter (464 nm/604 nm) to detect cells stained with PI. Eight images were collected at locations around the entire area of the sample membrane. Post-processing resulted in average percent cell viability counts for each image, which were then averaged for all eight images. The relative percent loss of viability for the pristine and fSWNTs are shown in Figure 2.

Representative fluorescent images. The following are representative images for two of the fSWNT samples.

Hydrazine SWNT **n-Propylamine SWNT**

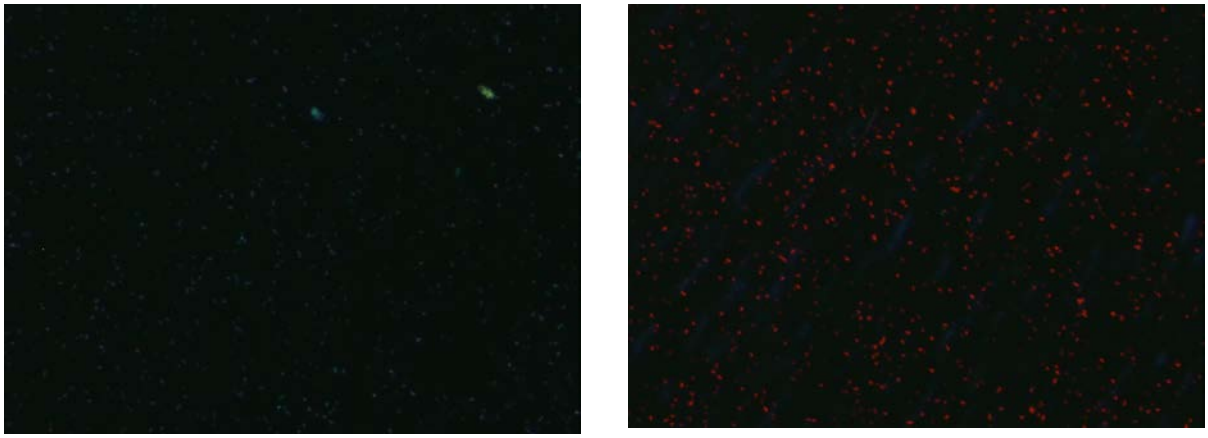

QikProp Descriptors: Brief descriptions of the descriptors and predicted properties from QikProp

 # stars: The number of violations of the 95% ranges for known drugs for the descriptors and predicted properties as indicated with *s in the propout file. Molecules with #stars > 0 are less drug-like.
 # amine: The count of non-conjugated amine groups.
 # amidine: The count of amidine and guanidine groups.
 # acid: The count of carboxylic acid groups.
 # amide: The count of non-conjugated amide groups.
 # rotor: The number of non-trivial (not CX3) non-hindered (not alkene, amide, small ring) rotatable bonds.
#rctvFG: The number of reactive functional groups; the specific groups are listed in the propout file. The presence of these groups can lead to false positives in HTS assays and to

decomposition/reactivity/toxicity problems in vivo.
CNS: The predicted central nervous system activity on a -2 (inactive) to +2 (active) scale.
MW: The molecular weight of the molecule.
dipole: The computed dipole moment for the molecule.
SASA: The total solvent-accessible surface area in Angstroms^2 using a probe with 1.4 Angstrom radius.
FOSA: The hydrophobic component of the SASA (saturated carbon and attached hydrogen).
FISA: The hydrophilic component of the SASA (SASA on N, O, and H on heteroatom).
PISA or ARSA: The pi (carbon and attached hydrogen) component of the SASA.
WPSA: The weakly polar component of the SASA (halogens, P, and S).
volume: The total solvent-accessible volume in Angstroms^3 using a probe with 1.4 Angstrom radius.
donorHB: The estimated number of hydrogen bonds that would be donated by the solute to water molecules in an aqueous solution.
accptHB: The estimated number of hydrogen bonds that would be accepted by the solute from water molecules in an aqueous solution.
dip^2/V: The (dipole moment)^2/molecular volume. Key term in the Kirkwood-Onsager eqution for the free energy of solvation of a dipole with volume V.
ACxDN^.5/SA or "ADOSA": accptHB*sqrt(donorHB)/volume - an index of cohesive interactions in solids; see Bioorg Med Chem Lett 10, 1155 (2000)
glob: The globularity descriptor = 4*pi*r^2/SASA where r is the radius of a sphere with a volume equal to the molecular volume. glob -> 1.0 for a spherical molecule.
QPpolrz: The predicted polarizability in Angstroms^3.
QPlogPC16: The predicted log of the hexadecane/gas partition coefficient.
QPlogPoct: The predicted log of the octanol/gas partition coefficient.
QPlogPw: The predicted log of the water/gas partition coefficient. Note: the solute's free energy of hydration = -2.3RT QPlogPw for gas phase -> water transfer.
QPlogPo/w: The predicted log of the octanol/water partition coefficient.
QPlogS: The predicted aqueous solubility, log S. S in moles/liter is the concentration of the solute in a saturated solution in equilibrium with the crystalline solid.
CIlogS: Alternative, conformation-independent prediction of aqueous solubility.
QPlogHERG: Predicted log IC50 for blockage of mammalian HERG K+ channels.
QPPCaco: The predicted apparent Caco-2 cell permeability in nm/sec.
QPPMDCK: The predicted apparent MDCK cell permeability in nm/sec - Affymax data.
QPlogBB: The predicted log of the brain/blood partition coefficient.
QPlogKp: The predicted log of the skin permeability.
IP(eV): The PM3 calculated ionization potential.
EA(eV): The PM3 calculated electron affinity.
 # metabol: The number of likely metabolic reactions that are listed in the QP.out file.
QPlogKhsa: The predicted log K'hsa for serum albumin binding.
HumanAbs: Predicted qualitative human oral absorption - 1, 2, or 3 for low, medium, or high.
QP%HumanAbs: Predicted human oral absorption on 0 to 100% scale.
SAfluorine: SASA for fluorines.
SAamideO: SASA for amide oxygens.
PSA: Polar (N and O) van der Waals surface area.
 # N and O: Number of nitrogens and oxygens.

Rule Of 5: Number of violations for Lipinski's rule of five.
 # ring atoms: Number of atoms in rings.
 # in 3 4: Number of atoms in 3 and 4-membered rings.
 # in 5 6: Number of atoms in 5 and 6-membered rings.
 # noncom: Number of atoms in rings that can not conjugate (e.g., 3 for cyclopentene).
 # non H atm: Number of non-hydrogen atoms.

Results and Discussion

Azo Coupling Byproduct of Phenyldicarboxy Functionalization. The presence of nitrogen and sulfur in SWNT-phenyldicarboxy **1i** (Figure 1), prepared by scaling up the method of [4], was unexpected. The treatment of SWNTs with diazonium salts has been described by others, but without any prior report of azo coupling byproducts (Figure S6) [16-18]. We considered the possibility of residual non-covalent contamination with unreacted starting material (5-aminoisophthalic acid), but this is unlikely due to the high efficiency of diazotization, the copious washing out of any acid soluble species (anilinium) and the subsequent organic washings (aniline) in the workup. Sayes et al. do not report any azo product from their preparation of **1i** starting with HiPCO SWNTs [4]. Although we used the same functionalization procedure, our starting material came from commercial CVD SWNTs purified by the manufacturer with an oxidizing acid treatment that introduces OH and CO_2H functionalities. Our starting material contained about 4.1% oxygen (Table 1). Formation of SWNT-amide (SWNT-CONHAr) or SWNT-ester (SWNT-O-COAr) is possible but unlikely and also not reported by others under a variety of diazotization conditions. The sub-stoichiometric AIBN used to catalyze the desired coupling forms isobutyryl nitrile free radical that could, in principle, react with SWNTs to form SWNT-$C(CH_3)_2CN$ but this also is unprecedented and seems less likely than alternatives.

On the basis of chemical reactivity, we feel the most likely nitrogenous byproduct formed under the reaction conditions is the azo coupling product as shown in Figure S6. Azo coupling is a very well known reaction in conventional non-SWNT chemistry [19]. Conventional azo coupling is pH dependent, being slower at low pH and faster at high pH. With SWNTs, pH adjustment might be used to increase the azo coupling yield from an impurity level to that of a major product to allow for better characterization. At this time, the only N-specific data is the XPS evidence of a C-N sigma bond in the sample. Our XPS data cannot distinguish C-N=N (azo) from starting material C-NH_2 (aniline) or other isomers. If the azo product has been formed, we believe this is the first report of such chemistry occurring on SWNTs and it invites further exploration of the phenomenon. Azo coupling could provide access to SWNTs with new, interesting, useful and tunable properties, such as electro-optical properties. E.g., enhanced visible light absorption by a suitable chromophore could result in direct electron injection into the SWNT. Azo dyes of general structure Ar-N=N-Ar' have been known for 150 years and it is only a small leap to consider SWNT-N=N-Ar' analogs. This chemistry is to be the subject of future research.

The presence of sulfur in sample **1i** is also unexpected. Although the reacted SWNTs are repeatedly resuspended in and filtered from DI water until the filtrates are neutral (to pH paper), it is possible that a trace of H_2SO_4 remains. In the case of partially oxidized CVD SWNTs (cf., HipCO SWNTs), it is possible that there is some O-sulfation to form SWNT-O-SO_3H or C-

sulphonylation to form SWNT-SO_3H at more reactive sites. Sulphonylation of coupled aromatic rings can occur as a byproduct of diazo coupling reactions in oleum. Our SWNT-Ph-SO_3H **1g** was prepared by sulphonylation of SWNT-Ph **1d** under similar oleum conditions [4].

There is also the possibility of intercalation of a small amount of SO_3 into the core of the tube. The van der Waals diameter of SO_3 (gas phase) is ~0.3 nm, small enough to fit inside some of the SWNTs with average tube diameters > 0.3 nm. XPS does not allow more detailed characterization of the sulfur impurity.

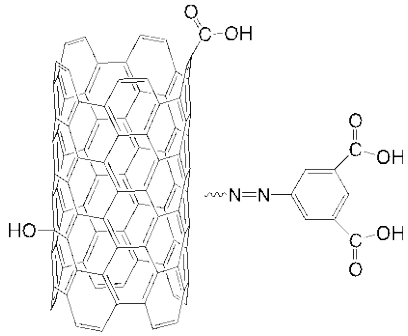

Figure S6. Molecular structure of the proposed azo coupling byproduct resulting from the synthesis of compound **1i**.

% Functionalization calculations. Approximate % functionalization calculations were performed using the XPS data (Table 1) for fSWNTs with functional groups containing identifiable elements (not carbon or hydrogen). Percent functionalization is a conventional measurement of the number of functional groups per tube backbone carbon and estimates the density of groups covalently bound to the SWNT. Due to the application of some assumptions, the details of the calculations performed are presented below. First, the atomic percent of carbon within the functional group is taken into account and subtracted from the total atomic percent carbon present in all samples. In the case of the hydroxy SWNTs, the total amount of oxygen present is assumed to be in the form of hydroxyl groups. For the phenyldicarboxy SWNT, the percent oxygen is used to determine the percent functionalization. We suspect that some of the oxygen present in the sample is directly bound to the tube in the form of hydroxyl and carboxyl groups. The amount present in the starting material, 4.1%, is used for a reasonable approximation and subtracted from the total percent oxygen present in the sample as detected by XPS.

<u>n-Propylamine</u>
0.6 at% N
1.8 at% C in the functional group (0.6 * 3C)
% functionalization = 0.6/(95.2 – 1.8) *100 = 0.64%
% functionalization = 0.6/93.4 *100 = 0.64%

<u>Phenylhydrazine</u>
0.8 at% N
0.8/2 = 0.4 at% N-N (correction for the two nitrogen atoms per functional group)
2.4 at% C in the functional group (0.4 * 6)
% functionalization = 0.4/93.3 *100 = 0.43%

Hydroxy
All oxygen is assumed to be in the form of hydroxy groups
% functionalization = 11.6/84.8 *100 = 13.7%

Phenyldicarboxy
19.9 at% O - 4.1 at% O on pristine tube = 15.8 at% oxygen assumed to be associated with the desired functional group, 4 oxygen atoms per group
15.8/4 = 3.95 (correction for the four oxygen atoms per functional group)
31.6 at% C in the functional group (3.95 * 8)
% functionalization = 3.95/46.2 *100 = 8.55%

We can correct for the presumed azo coupled $Ph(CO_2H)_2$ as follows:
1.92 at% N = 0.96 % azo (N=N)
0.96 * 8 C = 7.68 at% C ($N=NPh(CO_2H)_2$)
77.8 at% C total – 31.6 at% C in directly bound $Ph(CO_2H)_2$ – 7.68 at% C in azo bound $Ph(CO_2H)_2$ = 38.52 at% C in backbone
% direct $Ph(CO_2H)_2$ = 3.95 / 38.52 = 10.25 %
% azo $Ph(CO_2H)_2$ = 0.96 / 38.52 = 2.5 %
% total $Ph(CO_2H)_2$ = 12.75 %

The various assumptions provide reasonable upper and lower bounds for percent functionalization.

Sulfonic Acid
3.45 at% S was used to determine approximate percent functionalization
20.7 at% C in the functional group (3.45 * 6)
% functionalization = 3.45/57.4 *100 = 6.0%

Hydrazine
0.4 at% N
0.4/2 = 0.2 at% N (correction for the two nitrogen atoms per functional group)
% functionalization = 0.2/95.2 *100 = 0.21%

Statistical analysis of toxicity results. The cytotoxicity data was compiled using a standard box and whisker plot to show the relative median percent cell deaths and interquartile range (IQR = Q3-Q1). Whiskers were calculated as 1.5 x IQR. Two sample t-tests were performed to determine statistically significant differences between fSWNTs and the starting material. Two-tailed tests were performed with a 95% confidence interval and Welch's correction, due to unequal variance between the samples and starting material. Plots were made and statistical analysis performed in Prism (version 5.0d).

Table S1. QikProp output for the functional groups and chosen predicted properties.

	MW	dipole	QPlogPo/w	QPlogS	EA(eV)	PSA
n-propylamine	59.111	1.622	-0.167	1.771	-2.548	27.21
ph-hydrazine	108.143	3.446	0.149	0.78	-0.633	40.96
ph-(COOH)2	166.133	10.79	0.663	-1.27	1.24	99.22
phenyl	78.113	0	2.13	-1.641	-0.43	0
H2O (OH)	18.015	2.844	-1.38	1.274	-2.744	39.37
hydrazine	32.045	1.992	-2.776	2	-0.751	60.03
butyl	58.123	0.005	2.89	-2.57	-3.55	0
sulfonic acid	152.124	11.964	-1.336	1.316	5.153	58.56
DPCP	N/A	N/A	N/A	N/A	N/A	N/A

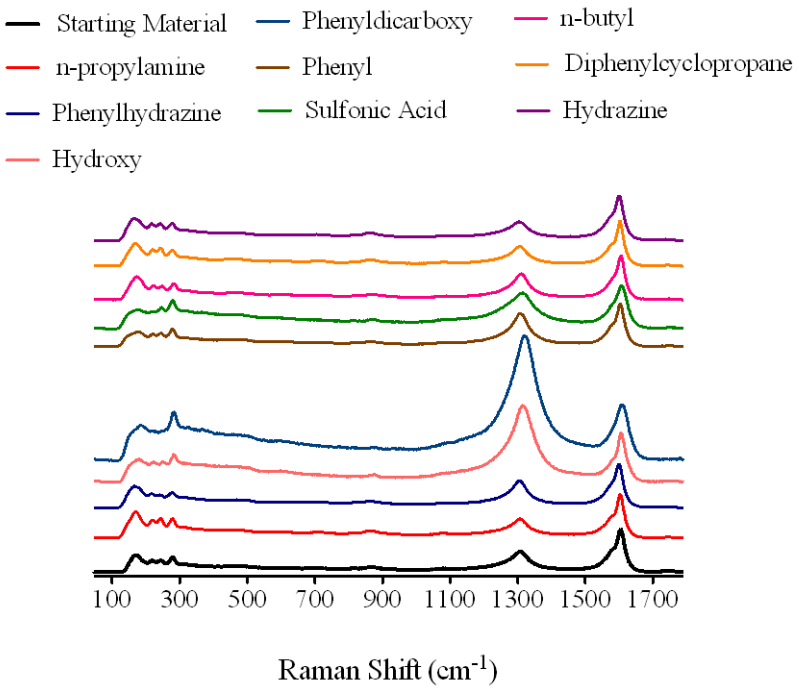

Sample	G:D
Starting Material	2.33
n-Propylamine	1.42
Phenylhydrazine	1.21
Hydroxy	0.87
Phenyldicarboxy	0.78
Phenyl	1.05
Sulfonic Acid	1.03
n-Butyl	1.29
Diphenylcyclopropane	1.19
Hydrazine	1.38

Figure S7: Raman spectra collected at 785 nm incident wavelength and normalized to the G-band. Spectra for each sample are normalized and averaged from five different locations on the bulk sample. Associated G:D ratios are calculated from the G and D-band peak intensities at ~1600 cm^{-1} and ~1300 cm^{-1}, respectively

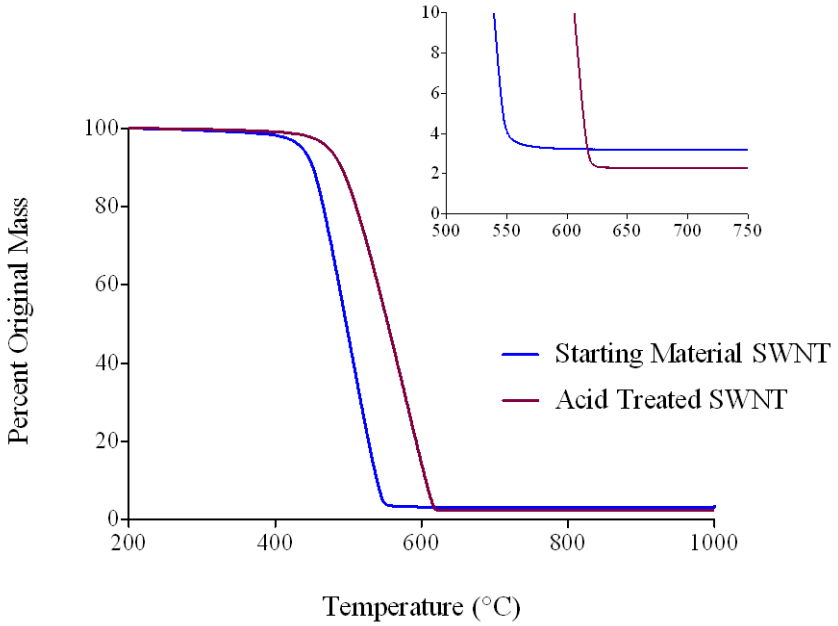

Figure S8: Thermogravimetric analysis of purchased SWNTs before and after acid treatment. The inset highlights the decrease in the percent residual after acid treatment.

Table S2: Burn off temperatures for pristine and fSWNTs were obtained from thermogravimetric analysis (TGA) rate of change of mass (DTG) curves. Tabulated temperatures are associated with maxima in the DTG curve.

Sample	Maximum Burn off Temperature(s) °C
Starting Material	579.3
n-Propylamine	335.0, 539.8
Hydroxy	383.4, 497.2
Phenyl Hydrazine	318.1, 471.4, 497.2
Phenyldicarboxy	357.7, 590.9
Phenyl	525.6
Sulfonic Acid	263.9, 346.6, 582.5
n-Butyl	332.3, 497.2, 530.9
Diphenylcyclopropane	443.0, 516.7
Hydrazine	315.0, 479.8

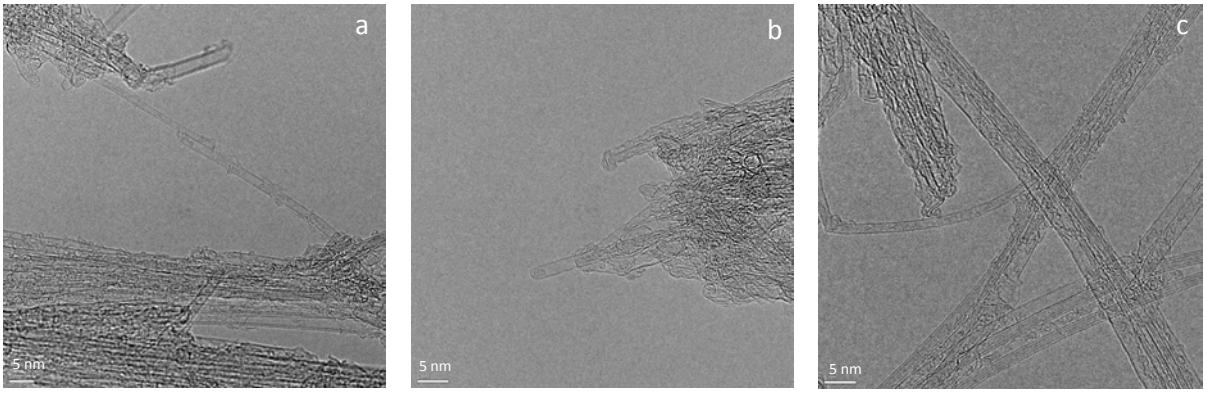

Figure S9: TEM images of a) starting material SWNT b) sulfonic acid SWNT and c) phenyl SWNT. Scale bars are all 5 nm.

Table S3: pH of fSWNT in 0.9% NaCl, the associated pKa values for functional group protons [20, 21], and the predicted dominant species present in solution. N-containing samples have two pK_a values associated with the conjugate acid and neutral form of the functional group. * indicates pK_a values obtained in DMSO.

Sample	pH	Estimated pKa	Dominant Species
Starting Material	6.61		
n-Propylamine	6.59	10.5, 30.6*	Conjugate acid (+)
Phenylhydrazine	6.67	5, 26.1*	Neutral
Hydroxy	6.67	9.95	Neutral
Phenyldicarboxy	6.94	4.2	Deprotonated (-)
Phenyl	6.67	43*	Neutral
Sulfonic Acid	6.62	1.9	Deprotonated (-)
n-Butyl	6.73	44*	Neutral
Diphenylcyclopropane	6.77	43*	Neutral
Hydrazine	6.67	8.1, 28*	Conjugate acid (+)

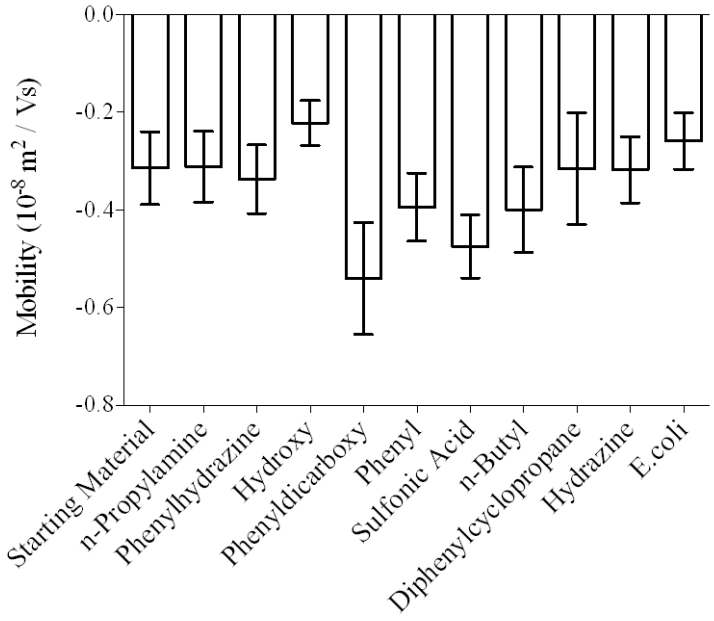

Figure S10: Electrophoretic mobility (EPM) of starting material, fSWNTs and *E. coli* dispersed in 0.9% NaCl.

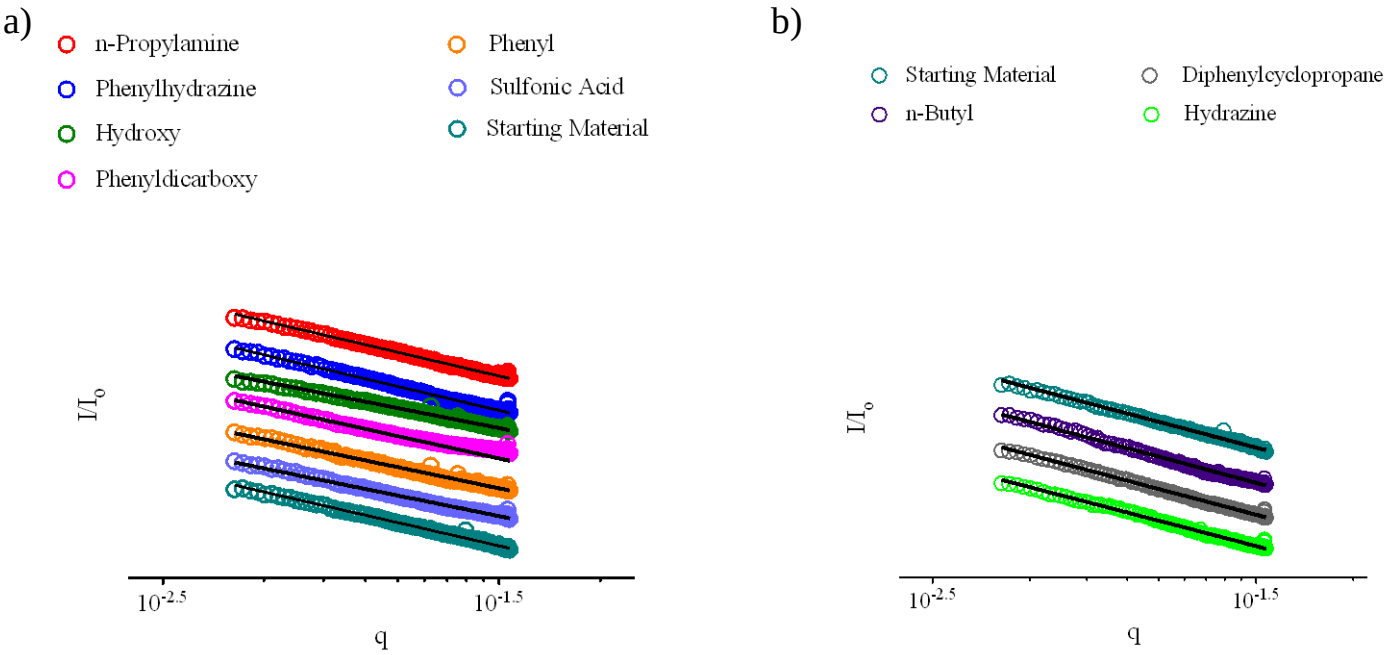

Figure S11. Plot of data collected by multi angle static light scattering (SLS). I/I_o vs q is plotted on a log-log scale for a) fSWNTs resulting in equal or increased loss in cell viability and b) fSWNTs resulting in decreased loss in cell viability compared with the starting material. The fractal dimensions (D_f) of each sample were extracted from the slope of their respective curves and compiled in Table S3. The magnitude of I/I_o in each of the sample curves has been adjusted for better data visualization.

Table S4. Fractal dimension values determined from the slope of the I/I_o vs q curves for the starting material and fSWNTs.

Sample	Fractal Dimension
n-Propylamine	2.79
Phenylhydrazine	2.82
Hydroxy	2.36
Phenyldicarboxy	2.63
Phenyl	2.49
Sulfonic acid	2.42
Starting Material	2.73
Butyl	2.78
Diphenylcyclopropane	2.74
Hydrazine	2.69

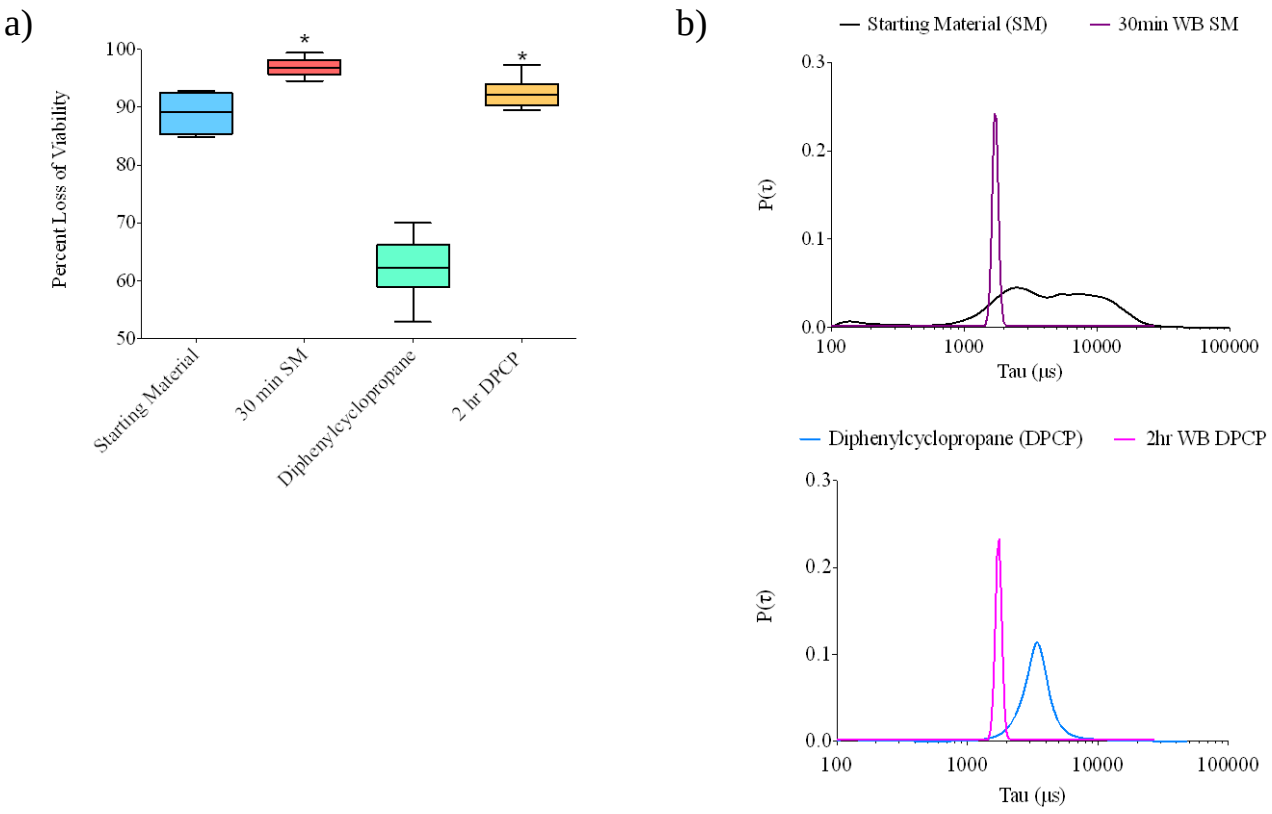

Figure S12. a) Box plot showing the comparative percent cell viability loss of the ball milled SWNT samples. Asterisk (*) indicates samples with a statistically significant difference in percent loss of cell viability compared with the starting material, determined by two-sample t-tests (95% CI, $\alpha = 0.05$). b) Normalized probability distributions of diffusion times (τ) for the starting material before and after treatment in the ball mill (upper) and diphenylcyclopropyl (DPCP) SWNT before and after treatment in the ball mill (lower).

1. Syrgiannis, Z.; Hauke, F.; Röhrl, J.; Hundhausen, M.; Graupner, R.; Elemes, Y.; Hirsch, A. Covalent Sidewall Functionalization of SWNTs by Nucleophilic Addition of Lithium Amides. *Eur. J. Org. Chem.* **2008,** (15), 2544-2550.
2. Pan, H.; Liu, L.; Guo, Z. X.; Dai, L.; Zhang, F.; Zhu, D.; Czerw, R.; Carroll, D. L. Carbon Nanotubols from Mechanochemical Reaction. *Nano Lett.* **2002,** *3* (1), 29-32.
3. Wunderlich, D.; Hauke, F.; Hirsch, A. Preferred functionalization of metallic and small-diameter single walled carbon nanotubes via reductive alkylation. *J. Mater. Chem.* **2008,** *18* (13), 1493-1497.
4. Sayes, C. M.; Liang, F.; Hudson, J. L.; Mendez, J.; Guo, W.; Beach, J. M.; Moore, V. C.; Doyle, C. D.; West, J. L.; Billups, W. E.; Ausman, K. D.; Colvin, V. L. Functionalization density dependence of single-walled carbon nanotubes cytotoxicity in vitro. *Toxicol. Lett.* **2006,** *161* (2), 135-142.
5. Peng, H.; Alemany, L. B.; Margrave, J. L.; Khabashesku, V. N. Sidewall Carboxylic Acid Functionalization of Single-Walled Carbon Nanotubes. *J. Am. Chem. Soc.* **2003,** *125* (49), 15174-15182.
6. Yokoi, T.; Iwamatsu, S.; Komai, S.; Hattori, T.; Murata, S. Chemical modification of carbon nanotubes with organic hydrazines. *Carbon* **2005,** *43* (14), 2869-2874.
7. Liu, C.; Zhang, Q.; Stellacci, F.; Marzari, N.; Zheng, L.; Zhan, Z. Carbene-Functionalized Single-Walled Carbon Nanotubes and Their Electrical Properties. *Small* **2011,** *7* (9), 1257-1263.
8. Avdoshenko, S. M.; Ioffe, I. N.; Sidorov, L. N. Smooth and Jump-like Metal-Dielectric Transitions in Single-Walled Carbon Nanotubes under Functionalization. *ACS Nano* **2010,** *4* (10), 6260-6266.
9. Bettinger, H. F. Addition of Carbenes to the Sidewalls of Single-Walled Carbon Nanotubes. *Chem. Eur. J.* **2006,** *12* (16), 4372-4379.
10. Wang, H.; Griffiths, J.; Egdell, R. G.; Moloney, M. G.; Foord, J. S. Chemical Functionalization of Diamond Surfaces by Reaction with Diaryl Carbenes. *Langmuir* **2008,** *24* (3), 862-868.
11. Mark, G. M. Functionalized polymers by chemical surface modification. *J. Phys. D: Appl. Phys.* **2008,** *41* (17).
12. Jonczyk, A.; Wlostowska, J. A Simple Method for Generation of Diazocompounds in an Aqueous Two-Phase System. *Synth. Commun.* **1978,** *8* (8), 569-572.
13. Kang, S.; Herzberg, M.; Rodrigues, D. F.; Elimelech, M. Antibacterial Effects of Carbon Nanotubes: Size Does Matter! *Langmuir* **2008,** *24* (13), 6409-6413.
14. Vecitis, C. D.; Zodrow, K. R.; Kang, S.; Elimelech, M. Electronic-Structure-Dependent Bacterial Cytotoxicity of Single-Walled Carbon Nanotubes. *ACS Nano* **2010,** *4* (9), 5471-5479.
15. Kang, S.; Pinault, M.; Pfefferle, L. D.; Elimelech, M. Single-Walled Carbon Nanotubes Exhibit Strong Antimicrobial Activity. *Langmuir* **2007,** *23* (17), 8670-8673.
16. Boul, P. J.; Nikolaev, P.; Sosa, E.; Arepalli, S. Potentially Scalable Conductive-Type Nanotube Enrichment Through Covalent Chemistry. *J. Phys. Chem. C.* **2011,** *115* (28), 13592-13596.
17. Dyke, C. A.; Stewart, M. P.; Maya, F.; Tour, J. M. Diazonium-based functionalization of carbon nanotubes: XPS and GC-MS analysis and mechanistic implications. *Synlett.* **2004,** (1), 155-160.

18. Mitchell, C. A.; Bahr, J. L.; Arepalli, S.; Tour, J. M.; Krishnamoorti, R. Dispersion of Functionalized Carbon Nanotubes in Polystyrene. *Macromolecules* **2002,** *35* (23), 8825-8830.
19. Zollinger, H. *Diazo Chemistry 1: Aromatic and Heteroaromatic Compounds*; Wiley-VCH Verlag GmbH & Co. KGaA: New York, 1994.
20. Jenks, W. P.; Westheimer, F. H., pKa Data Compiled by R. Williams. In *research.chem.psu.edu/brpgroup/pKa_compilation.pdf* (accessed May 15, 2011).
21. Ripin, D. H.; Evans, D. A., pKa Table. In *evans.harvard.edu/pdf/evans_pKa_table.pdf*, 2005 (accessed May 15, 2011).